Effects of convective ice evaporation on interannual variability of tropical tropopause layer water vapor

Hao Ye, Andrew E. Dessler, and Wandi Yu

Department of Atmospheric Sciences, Texas A&M University, College Station, USA

Correspondence to: Andrew E. Dessler (adessler@tamu.edu)

Abstract.

Water vapor interannual variability in the tropical tropopause layer (TTL) is investigated using satellite observations and model simulations. We breakdown the influences of the Brewer-Dobson circulation (BDC), the quasi-biennial oscillation (QBO), and the tropospheric temperature (ΔT) on TTL water vapor as a function of latitude and longitude using a 2-dimensional multivariable linear regression. This allows us to examine the spatial distribution of the impact on TTL water vapor from these physical processes. In agreement with expectation, we find that the impacts from the BDC and QBO act on TTL water vapor by changing TTL temperature. For ΔT, we find that TTL temperatures alone cannot explain the influence. We hypothesize a moistening role for the evaporation of convective ice from increased deep convection as the troposphere warms. Tests using a chemistry-climate model, the GEOSCCM, support this hypothesis.

1 Introduction

Stratospheric water vapor plays an important role in both the chemistry (Stenke and Grewe, 2005) and radiative energy budget (Solomon et al., 2010; Dessler et al., 2013) of the atmosphere. Air enters the stratosphere from the tropical troposphere mainly through the tropical tropopause layer (TTL, $\sim$15-18 km) (Sherwood and Dessler, 2000; Fueglistaler et al., 2009), which serves as a transition region between the troposphere and stratosphere. It is generally recognized that the coldest temperatures in the TTL act like a "cold trap" that provides primary control on the amount of water vapor entering the lower stratosphere (Mote et al., 1996; Holton and Gettelman, 2001). Large interannual variations of TTL water vapor have been observed and attributed to a set of physical processes that affect water vapor by varying TTL temperatures, such as the quasi-biennial oscillation (QBO) (Geller et al., 2002; Fueglistaler and Haynes, 2005; Liang et al., 2011; Liess and Geller, 2012; Randel and Jensen, 2013; Wang et al., 2015; Tao et al., 2015) and the Brewer-Dobson circulation (BDC) (Randel et al., 2006; Calvo et al., 2010; Dessler et al., 2013, 2014; Fueglistaler et al., 2014; Gilford et al., 2016).

Another important process is the deep convection that reaches the TTL. Clouds comprised of convective ice can have important impacts on planetary energy balance (Lee et al., 2009; Zhou et al., 2014), and their evaporation can moisten the TTL (Corti et al., 2008; Wang and Dessler, 2012). The efficiency of cloud evaporation is strongly related to ambient relative humidity (Dessler and Sherwood, 2004; Wright et al., 2009) because high relative humidity inhibits evaporation. Recent aircraft measurements (Anderson et al., 2012; Herman et al., 2017) and satellite observations (Dessler and Sherwood, 2004; Schwartz et al., 2013; Sun and Huang, 2015) confirm that the deep convection enhances lower stratospheric water vapor over the North American summer monsoon region, where relative humidity is very low.

In the tropics, the influence of convection on observed water vapor amounts is less clear. It seems certain that convective ice evaporation at least occasionally moistens the stratosphere (Khaykin et al., 2009; Hassim and Lane, 2010; Carminati et al., 2014; Frey et al., 2015; Virts and Houze Jr, 2015), but the impact of convection there is muted because the relative humidity of the TTL is high, suppressing evaporation, and only convection reaching above the cold point is likely to significantly impact the humidity of the stratosphere (Dessler et al., 2007).

Several modeling studies have addressed this by adding convection moistening into the trajectory model simulation, through a convective probability scheme (Dessler et al., 2007; Schoeberl and Dessler, 2011) or a reanalysis-based anvil ice scheme (Schoeberl et al., 2014) or an observation-based convective cloud top scheme (Ueyama et al., 2014, 2015). All these model simulations are in agreement that the convective ice can moisten the TTL and lower stratosphere. Schoeberl et al. (2014) and Ueyama et al. (2015) estimated that convective ice evaporation increases TTL water vapor by 0.3 ppmv and 0.5 to 0.6 ppmv, respectively. In addition, a recent case study has shown that evaporation of convective ice could account for a significant part of the TTL water vapor response to the strong El Niño of 2015-2016 (Avery et al., 2017).

On longer time scales, the impact of ice evaporation on stratospheric water vapor could be much more important. Almost all climate models predict that the water vapor in the UTLS will increase over the next century(Gettelman et al., 2010), and a significant fraction of this increase was found to be due to the evaporation of convective ice from convection in two chemistry-climate models (Dessler et al., 2016). This gives us ample motivation to look more closely at the impact of convective ice evaporation on TTL water vapor in the observations.

The purpose of this study is to investigate in more detail the physical processes controlling the interannual variations of water vapor in the TTL, particularly the influence of evaporation of convective ice. Previous work has mostly taken a “forward model” approach — where a model (usually a dynamical model coupled to a microphysical model) driven by observations of winds, temperatures, and convection, is used to make an explicit estimate of the convective influence. Our analysis takes a different approach — we use a statistical model to decompose the water vapor variability into the dominant physical processes known to drive water vapor. We do this in both observations and water vapor simulated by a trajectory model. Because the trajectory model does not include convection, differences in the results will be tied to the influence of convection. We verify the methodology by reproducing it in a chemistry-climate model with known convection.

2 Data and Methods

2.1 MLS water vapor

The observations of TTL water vapor are from the Earth Observing System (EOS) Aura Microwave Limb Sounder (MLS) (Lambert et al., 2007; Read et al., 2007). The MLS instrument has obtained continuous high-quality global observations of water vapor in the upper troposphere and stratosphere since August 2004. The data is available from https://mls.jpl.nasa.gov/.

Here we use MLS version 4.2 level 2 water vapor retrievals from August 2004 to December 2016. The daily water vapor mixing ratio measurements are binned and averaged to produce monthly data on a $4^\circ \times 8^\circ$ latitude and longitude grid with the quality control following the instruction in Livesey et al. (2017). We focus on the interannual anomalies of water vapor from 30°N to 30°S at 100 hPa. Throughout this paper, the interannual anomalies at each grid point are calculated by subtracting the average annual cycle at that grid point.

2.2 GEOSCCM

We also use simulations of TTL water vapor from the Goddard Earth Observing System Chemistry Climate Model (GEOSCCM) in this study. The state-of-the-art GEOSCCM includes the GEOS-5 atmospheric general circulation model (Molod et al., 2012) with a single-moment cloud microphysics scheme (Bacmeister et al., 2006; Barahona et al., 2014) and the StratChem stratospheric chemical mechanism (Pawson et al., 2008; Oman and Douglass, 2014). The GEOSCCM simulation provides long term simulations of temperature, water vapor, horizontal winds, diabatic heating rates, and convective ice with a resolution of $2^\circ \times 2.5^\circ$ in latitude and longitude on 72 vertical model levels, up to 0.01 hPa.

In this study, we investigate the water vapor simulated by the GEOSCCM in the TTL during model years corresponding to the MLS period. As these simulations are from a free-running model, climate variability in the model is not synchronous with that in the observations, so the comparisons with MLS observations are done statistically — using regression models (discussed below).

2.3 Trajectory model

We also produce simulations of TTL water vapor using a domain-filling forward trajectory model, which has been in previous work to reproduce water vapor, ozone, and carbon monoxide anomalies in the TTL and lower stratosphere (Schoeberl and Dessler, 2011; Schoeberl et al., 2012, 2013; Dessler et al., 2014; Wang et al., 2014).

This model uses Bowman's trajectory code (Bowman, 1993; Bowman and Carrie, 2002). The parcels are driven by 6-hourly horizontal winds and total diabatic heating rates from either reanalysis datasets or from the GEOSCCM. When comparing to MLS data, we use trajectory runs driven by two reanalysis datasets: the European Centre for Medium-Range Weather Forecasts (ECMWF) ERA-interim reanalysis (ERAi) (Dee et al., 2011) and the NASA's Modern-Era Retrospective-Analysis for Research and Applications Version-2 (MERRA-2) (Bosilovich et al., 2016). When comparing to GEOSCCM output, we drive the model with meteorological fields from the GEOSCCM.

In all simulations, 1350 parcels are initialized every day from January 2000 to December 2016 on an equal area grid from 60°N to 60°S. The parcels are released on the 370-K isentropic level, which is just above the zero net diabatic heating level over the tropics (∼355-360 K) but below the cold point (∼375-380 K). Each parcel travels forward following the horizontal winds and diabatic heating rate. Once a parcel has a pressure larger than 250 hPa, it is regarded as having descended back into the troposphere and is removed from the model.

Each parcel is initialized with a water vapor mixing ratio of 200 parts per million by volume (ppmv). Along the trajectory, a parcel will immediately be dehydrated to saturation once its water vapor mixing ratio exceeds a predetermined saturation threshold, 100% in this study. The saturated water vapor mixing ratio is obtained from the thermodynamic equation with respect to ice (Murphy and Koop, 2005) based on temperatures from reanalyses or the GEOSCCM. The production of water vapor from methane oxidation is also included in these trajectory model runs but it has very little effect on water vapor in the TTL (Dessler et al., 2014).

The water vapor mixing ratio from the trajectory model is gridded into $4° \times 8°$ bins, just as the MLS data were. In the vertical, the trajectory output is binned by averaging the parcels in a pressure range around each MLS or GEOSCCM level. In comparisons to MLS, the gridded water vapor mixing ratio is then re-averaged using the MLS averaging kernels following the instruction from Livesey et al. (2017). When doing this kernel averaging, grid boxes with no trajectory parcels (mostly at low altitudes) are filled with monthly water vapor mixing ratios from the reanalyses (ERAi and MERRA-2). Sensitivity tests confirm that changing water vapor mixing ratio from the reananlyses has no impact on the spatial distribution of the interannual variability of TTL water vapor that is the focus of this paper.

2.4 Convection clouds

We also use estimates of convective cloud occurrence produced by combining geostationary infrared satellite imagery and microwave rainfall measurements (Pfister et al., 2001; Bergman et al., 2012; Ueyama et al., 2014, 2015). The data have a horizontal resolution of $0.25° \times 0.25°$ and a temporal resolution of 3 hours and cover the period from 2005 to 2016. In this paper, we use the cloud-top height and cloud-top potential temperature to estimate the convective cloud occurrence frequency in the TTL, which we take to be an indicator of convective influence on the TTL. These data are available from https://bocachica.arc.nasa.gov/~lpfister/cloudtop/.

3 Results

3.1 Influence of the BDC and QBO on TTL water vapor

Fig. 1 shows monthly and tropical averaged 100-hPa H_2O anomalies from MLS observations and from trajectory model runs driven by meteorology from ERAi (traj_ERAi) and MERRA-2 (traj_MERRA2). Similar to the results in Dessler et al. (2013, 2014) at 82 hPa, there is good agreement between the observations and trajectory models at 100 hPa.

Dessler et al. (2013, 2014) also showed that we can fit tropical average anomalies of 82 hPa H_2O with a simple linear model:

$$\mathrm{H_2O} = a \cdot \mathrm{BDC} + b \cdot \mathrm{QBO} + c \cdot \Delta T + r, \quad (1)$$

where BDC, QBO, and ΔT are indices representing the strength of the Brewer-Dobson circulation, the phase of the QBO, and the tropospheric temperature anomalies of the tropical climate system, respectively. Smalley et al. (2017) verified this approach is also valid in chemistry-climate models.

To gain additional physical insight into that result, in this paper we perform a similar multivariable regression, but at individual grid points in the TTL:

$$H_2O(x_i, y_j) = a(x_i, y_j) \cdot \mathrm{BDC} + b(x_i, y_j) \cdot \mathrm{QBO} + c(x_i, y_j) \cdot \Delta T + r(x_i, y_j). \quad (2)$$

Here, $H_2O(x_i, y_j)$ represents the H_2O anomaly time series at 100 hPa in a grid-box centered at longitude x_i and latitude y_j. The coefficients a, b, and c, as well as the residual term r, are also functions of latitude and longitude.

The regressors in Eq. 2 are the same tropical average time series used in Dessler et al. (2013, 2014): BDC is a Brewer-Dobson circulation index — here we use the tropical averaged diabatic heating rate anomaly at 82 hPa, with units of $\mathrm{K\ day^{-1}}$. QBO is a quasi-biennial oscillation index and here we use standardized monthly and zonally averaged equatorial zonal winds anomaly at 50 hPa, with units of $\mathrm{m\ s^{-1}}$. ΔT is tropical averaged tropospheric temperature anomaly at 500 hPa, with units of degrees K. Because these regressors are tropical average values, they do not vary with location. The QBO index is lagged by 2 months in the regression because the phase of the QBO takes time to impact TTL temperature and then the water vapor at 100-hPa (Dessler et al., 2013). There is no lag for the BDC and ΔT indices in this study.

We first analyze MLS H_2O observations. We run the regression on these observations twice: once using BDC and ΔT regressors from the ERAi reanalysis and again using regressors from the MERRA-2 reanalysis. The QBO index is the same in both regressions (we use observations downloaded from http://www.cpc.ncep.noaa.gov/data/indices/qbo.u50.index).

The BDC coefficients (Figs. 2a and 2d) are negative over the tropics, consistent with the idea that an enhanced Brewer-Dobson Circulation cools the TTL (Yulaeva et al., 1994; Randel et al., 2006) and reduces water vapor (Dhomse et al., 2008). The QBO coefficients (Figs. 3a and 3d) are positive over almost all of the tropics, as the positive phase of QBO tends to decrease the upwelling in TTL, thereby warming it (Plumb and Bell, 1982; Davis et al., 2013).

We also run the regression on H_2O simulated by the trajectory model. We use BDC and ΔT regressors from the same reanalysis used to drive each trajectory model (i.e., we use ERAi regressors to analyze the ERAi-driven trajectory model); the QBO index is always from the NCEP observations.

The BDC coefficients from regression of the trajectory models (Figs. 2b and 2e) agree well with the coefficients from the regressions of the MLS observations. The gridpoint-by-gridpoint scatter plots (MLS vs. trajectory; Figs. 2c and 2f) demonstrate this agreement in more detail. The only clear difference is that the regression of the MLS data using MERRA-2 regressors produces BDC coefficients that tend to be more negative than those from the trajectory model driven by MERRA-2 meteorology. This stems from what appear to be problems in the MERRA-2 heating rates. These heating rates disagree significantly with those from both ERAi as well as the original MERRA. While this has a minor effect on water vapor predicted by the trajectory model, it does have a large impact on regressions that use heating rates as a regressor.

The QBO coefficients from the regressions of the trajectory models are shown in Figs. 3b and 3e with gridpoint-by-gridpoint scatter plots in Figs. 3c and 3f. As with the BDC comparison, the trajectory models do a good job reproducing the regressions of the MLS data.

Overall, we conclude that the trajectory model accurately captures the impact of the BDC and QBO on TTL water vapor — for both the tropical average and the spatial distribution. This supports the hypothesis that these processes mainly influence

TTL water vapor by varying large-scale TTL temperatures and transport (Giorgetta and Bengtsson, 1999; Randel et al., 2000; Geller et al., 2002; Randel et al., 2006; Dhomse et al., 2008; Liang et al., 2011; Davis et al., 2013; Dessler et al., 2013, 2014; Wang et al., 2015), which we expect the trajectory model to reproduce.

3.2 Influence of tropospheric temperature on TTL water

Coefficients of ΔT from the MLS regressions are mostly positive, with large increases over the Tropical Warm Pool region (TWP) and Indian Ocean (Figs. 4a and 4e), indicating that warming of the tropical troposphere increases TTL water vapor mixing ratio there. Over the Central Equatorial Pacific (CEP), however, a warming troposphere *decreases* water vapor.

The decrease in water vapor in the CEP is not entirely unexpected. TTL temperatures are usually coldest — and water vapor a minimum — above the convection maximum in the TWP. As ΔT increases in response to an El Niño event, this convective maximum, and its associated TTL cold pool, shifts eastward from the TWP to the CEP (corresponding to a shift from Figs. 5a and 5b) (Davis et al., 2013; Hu et al., 2016; Konopka et al., 2016; Avery et al., 2017). Changes in TTL H_2O are expected to mirror this, with increases in water vapor in the TWP and decreases in the CEP as ΔT increases.

Both the MLS and trajectory model regressions show this dipole pattern. However, the MLS regressions yield ΔT coefficients that are systematically higher than those found in the trajectory regressions throughout the tropics (Figs. 4c and 4f). For the MLS/ERAi comparison (Fig. 4c), the average coefficients are 0.43 $\mathrm{ppmv\ K^{-1}}$ and 0.28 $\mathrm{ppmv\ K^{-1}}$; for the MLS/MERRA-2 comparison (Fig. 4f), the average coefficients are 0.20 $\mathrm{ppmv\ K^{-1}}$ and 0.05 $\mathrm{ppmv\ K^{-1}}$. We have also done regressions using tropical average values (using Eq. 1, similar to what was done in Dessler et al. (2013, 2014)) and find that the ΔT coefficients from MLS and trajectory models are statistically different with probabilities of 85% and 70% for ERAi and MERRA-2, respectively. This probability is the chance that the two ΔT coefficient probability distributions from MLS and trajectory models are not the same.

We hypothesize that the evaporation of convective ice accounts for the difference between the ΔT coefficients in the MLS and trajectory-model regressions. As convection moves eastward during an El Niño event (Figs. 5a and 5b), there is an accompanying increase in convective ice in the TTL (Avery et al., 2017), where it evaporates and hydrates the TTL. The moistening from evaporation spreads throughout the tropics and increases the water vapor everywhere. The trajectory model, which does not include this process, simulates a smaller increase in water vapor, leading to smaller ΔT coefficients (Figs. 4c and 4f).

In support of this, in Fig. 6a we show that the tropical averaged convective cloud occurrence frequency anomalies at 370 K increase with ΔT. This is consistent with the hypothesis that, as ΔT increases, we should also see an increase in evaporation of cloud ice.

3.3 Tests with a climate model

To gain additional confidence in our hypothesis that evaporation of convective ice plays a role in the TTL water budget, we perform a parallel analysis with the GEOSCCM, a model where evaporation of convective ice is known to add water to the TTL (Dessler et al., 2016). To do this, we run regression on the GEOSCCM 100-hPa H_2O fields as well as on H_2O simulated by a trajectory model driven by the GEOSCCM meteorology.

Figs. 2g and 2h show the spatial distribution of the BDC coefficients from the GEOSCCM and the corresponding trajectory model. This comparison is analogous to the comparison of the regressions on the MLS data and trajectory models driven by reanalyses. The coefficients are similar to each other and to the MLS regressions, suggesting that the GEOSCCM is accurately simulating the impact of BDC changes on TTL water vapor. The influence of the QBO in the version of the GEOSCCM analyzed here does not extend into the TTL, so we have not included a QBO term in the regression and there are consequently no GEOSCCM QBO coefficients in Fig. 3.

Before we discuss the ΔT coefficients, it is worth pointing out that the GEOSCCM has realistic ENSO variability in TTL temperatures and convective ice. Figs. 5c and 5d show that the monthly convective cloud ice water content (IWC) anomalies at 118 hPa and cold anomalies at 100 hPa in the GEOSCCM shift eastward as the ΔT warms from a cold phase (Fig. 5c) to a warm phase (Fig. 5d), just as they did in observations (Figs. 5a and 5b).

The ΔT coefficient fields from the GEOSCCM and associated trajectory regressions (Figs. 4g and 4h) show the same structural differences as do the ΔT coefficients from the MLS and accompanying trajectory-model regressions — that the ΔT coefficient is larger in the GEOSCCM regression than in the trajectory-model regression; the tropical average ΔT coefficients from GEOSCCM and trajectory model are significantly different at the 85% confidence level. In the last section, we hypothesized that this difference in the coefficients was due to evaporation of convective ice in the MLS data, a process not included in the trajectory model.

To directly test this hypothesis in the GEOSCCM, we run a second version of the trajectory model that includes the evaporation of convective ice from GEOSCCM, referred to hereafter as traj_ccm_ice. To do this, we use the 6-hourly three-dimensional convective cloud IWC field from GEOSCCM and linearly interpolate it to each parcel's position at every time step. We then assume instantaneous and complete evaporation of this ice into the parcel by adding the IWC to the parcel's water vapor, although we do not let parcels exceed 100% relative humidity with respect to ice. This is the same procedure used to simulate convective ice evaporation by Dessler et al. (2016) .

We then run the regression on the traj_ccm_ice's H_2O field. The scatter plot of GEOSCCM vs. traj_ccm_ice BDC coefficients (Fig. 2k) shows larger scatter than the comparison without ice (Fig. 2i). The increase in scatter is likely the result of the crudeness of our microphysical assumptions, particularly the assumption that convective ice evaporates instantaneously. However, the comparison between the tropical average GEOSCCM BDC coefficient, -6.2 $\mathrm{ppmv}\ (\mathrm{K\ day^{-1}})^{-1}$, and those from the trajectory models, -5.8 and -6.9 $\mathrm{ppmv}\ (\mathrm{K\ day^{-1}})^{-1}$ without and with convective ice evaporation, respectively, is similar.

The scatter plot of GEOSCCM vs. traj_ccm_ice ΔT coefficients (Fig. 4k) similarly shows larger scatter than the comparison without ice (Fig. 4i). Adding ice does, however, increase the average ΔT coefficient (seen by comparing Figs 4i to 4k), from $0.16\ \mathrm{ppmv\ K^{-1}}$ to $0.32\ \mathrm{ppmv\ K^{-1}}$, bringing the trajectory model into closer agreement with the GEOSCCM, which has a corresponding value of $0.31\ \mathrm{ppmv\ K^{-1}}$. There are also some interesting changes in the spatial pattern of the traj_ccm_ice (Fig. 4j). For example, negative ΔT coefficients appear in the TWP and Indonesia in the traj_ccm_ice regression; The cause of this is unknown, but also is likely linked to the trajectory model's ice evaporation assumption.

We showed in the previous section that the convective cloud occurrence frequency in the TTL increased as ΔT increased (Fig. 6a) and we also see that the GEOSCCM simulates a similar correlation between convective cloud IWC and ΔT (Fig. 6b).

While these are not exactly the same quantity, they show a consistency that provides confidence that the behavior of the model is realistic.

Finally, to quantify convective ice evaporation, we calculate the evaporation rate of convective ice at 100 hPa in the trajectory model. To do this, we save the amount of water added to each parcel by ice evaporation in every time step. We then bin and average the amount evaporated to come up with the distribution of the amount evaporated per day. Note that much of this water added will be lost in subsequent dehydration events, so this does not represent net water added to the stratosphere.

Fig. 6c shows that the tropical average evaporation rate of convective ice also increases with ΔT, which provides further evidence that the difference in ΔT coefficients between the GEOSCCM and the trajectory model is due to evaporation of convective ice. Fig. 7 shows the distribution of monthly averaged evaporation rate during ENSO-like warm and cold phases in the GEOSCCM. We see that, as ΔT increases and we transition from a cold to warm phase of variability, the location of ice evaporation shifts from the TWP and Indian Ocean to the CEP. This is consistent with the analysis of Avery et al. (2017).

4 Conclusions

Previous work has shown that TTL water vapor variability is mainly controlled by TTL temperature variability (Mote et al., 1996; Holton and Gettelman, 2001; Fueglistaler et al., 2009). In particular, variations in the Brewer-Dobson circulation (BDC) and the quasi-biennial oscillation (QBO) play key roles (Fueglistaler and Haynes, 2005; Geller et al., 2002; Liang et al., 2011; Liess and Geller, 2012; Calvo et al., 2010; Randel et al., 2006; Dessler et al., 2013, 2014; Tao et al., 2015). It has been suggested by many previous investigators that evaporation of convective ice may also contribute water to the TTL (Khaykin et al., 2009; Hassim and Lane, 2010; Carminati et al., 2014; Frey et al., 2015; Virts and Houze Jr, 2015; Schoeberl and Dessler, 2011; Schoeberl et al., 2014; Ueyama et al., 2014, 2015; Dessler et al., 2016; Avery et al., 2017). In this paper, we analyze the spatial distribution of TTL water vapor and conclude that, indeed, convection makes a small contribution to the interannual variability over the MLS period.

To do that, we use a linear regression model on TTL water vapor at individual grid points over the tropics to investigate the spatial distribution of the impact of the BDC, QBO, and tropospheric temperature (ΔT). We run this linear regression model on MLS observations of TTL water vapor anomalies and on water vapor anomalies simulated by a trajectory model that only includes the effects of TTL temperatures on water vapor.

The spatial pattern and magnitude of the BDC and QBO coefficients agree well between MLS observations and associated trajectory model simulations. This suggests that, consistent with expectations, these processes affect TTL water vapor mainly by changing TTL temperatures (Randel et al., 2000; Geller et al., 2002; Randel et al., 2006; Dhomse et al., 2008; Liang et al., 2011; Davis et al., 2013; Dessler et al., 2013, 2014).

The spatial distribution of ΔT coefficients has an obvious dipole structure associated with the ENSO (Konopka et al., 2016): negative values in the Central Equatorial Pacific (CEP), where temperatures decrease as the troposphere warms, and positive values in the Tropical Warm Pool (TWP), where the opposite occurs.

We also find that ΔT coefficients from the MLS observations are larger throughout the tropics than in the trajectory model. We hypothesize that changes in convection as ΔT increases leads to increases in evaporation of convective ice in the TTL. This increases the ΔT coefficient in the MLS analysis, but not in the trajectory model, which does not have convective ice evaporation in it. We see support for this in the observations of increased convective cloud occurrence frequency in the TTL as ΔT increases. This result is also in agreement with the case study in Avery et al. (2017) as well as the model analysis in Schoeberl and Dessler (2011), Schoeberl et al. (2014), and Ueyama et al. (2014, 2015).

To gain additional confidence in our hypothesis that evaporation of convective ice is responsible for the difference in ΔT coefficients, we test the methodology in a parallel analysis with the GEOSCCM, a model where evaporation of convective ice is known to add water to the TTL (Dessler et al., 2016). We find that the results of this analysis show the same difference — that the ΔT coefficients from the regression of the GEOSCCM's water vapor field are larger than the coefficients from a trajectory model driven by GEOSCCM meteorology.

We confirm this is due to evaporation of convective ice by running a second version of the trajectory model, which includes convective ice evaporation. We find that the ΔT coefficient from the regression of this version of the trajectory model is in agreement with that from the GEOSCCM regression.

Putting all of these together, we conclude that variability in the evaporation of convective ice plays a role in water vapor variability in the TTL. Our work should not be taken as opposing previous research (Randel et al., 2006; Schiller et al., 2009; Wright et al., 2011; Randel and Jensen, 2013) that concluded most of the variance in TTL water vapor over the last few decades is due to TTL temperatures. We concur that the impact of convective ice only is a minor contributor to TTL water vapor variability over the period spanned by the MLS data. But for GEOSCCM, which does an excellent job simulating TTL water vapor over the comparable period, suggests that convective ice may play a much larger role in long-term trends of TTL and stratospheric water vapor (Dessler et al., 2016), so more research on this phenomenon is clearly warranted.

Competing interests. The authors declare that they have no conflict of interests.

Acknowledgements. We thank Mark Schoeberl for his insights into this problem. This work was supported by NASA grant NNX14AF15G to Texas A&M University. We would like to thank Luke Oman and Anne Douglass for providing the simulation of GEOSCCM used in this study, the modeling effort is supported by the NASA MAP program and the high-performance computing resources that were provided by the NASA Center for Climate Simulation (NCCS).

References

Anderson, J. G., Wilmouth, D. M., Smith, J. B., Sayres, D. S., et al.: UV dosage levels in summer: Increased risk of ozone loss from convectively injected water vapor, Science, 337, 835–839, 2012.

Avery, M. A., Davis, S. M., Rosenlof, K. H., Ye, H., and Dessler, A. E.: Large anomalies in lower stratospheric water vapour and ice during the 2015-2016 El Niño, Nature Geoscience, 10, 405–409, 2017.

Bacmeister, J. T., Suarez, M. J., and Robertson, F. R.: Rain reevaporation, boundary layer–convection interactions, and Pacific rainfall patterns in an AGCM, Journal of the Atmospheric Sciences, 63, 3383–3403, 2006.

Barahona, D., Molod, A., Bacmeister, J., Nenes, A., Gettelman, A., Morrison, H., Phillips, V., and Eichmann, A.: Development of two-moment cloud microphysics for liquid and ice within the NASA Goddard Earth Observing System Model (GEOS-5), Geoscientific Model Development, 7, 1733–1766, 2014.

Bergman, J. W., Jensen, E. J., Pfister, L., and Yang, Q.: Seasonal differences of vertical-transport efficiency in the tropical tropopause layer: On the interplay between tropical deep convection, large-scale vertical ascent, and horizontal circulations, Journal of Geophysical Research: Atmospheres, 117, 2012.

Bosilovich, M., Lucchesi, R., and Suarez, M.: MERRA-2: File specification, GMAO Office Note No. 9 (Version 1.1), Tech. Rep. Version 1.1, Global Modeling and Assimilation Office, 2016.

Bowman, K. P.: Large-scale isentropic mixing properties of the Antarctic polar vortex from analyzed winds, Journal of Geophysical Research: Atmospheres, 98, 23 013–23 027, 1993.

Bowman, K. P. and Carrie, G. D.: The mean-meridional transport circulation of the troposphere in an idealized GCM, Journal of the Atmospheric Sciences, 59, 1502–1514, 2002.

Calvo, N., Garcia, R., Randel, W., and Marsh, D.: Dynamical mechanism for the increase in tropical upwelling in the lowermost tropical stratosphere during warm ENSO events, Journal of the Atmospheric Sciences, 67, 2331–2340, 2010.

Carminati, F., Ricaud, P., Pommereau, J.-P., Rivière, E., Khaykin, S., Attié, J.-L., and Warner, J.: Impact of tropical land convection on the water vapour budget in the tropical tropopause layer, Atmospheric Chemistry and Physics, 14, 6195–6211, 2014.

Corti, T., Luo, B., De Reus, M., Brunner, D., Cairo, F., Mahoney, M., Martucci, G., Matthey, R., Mitev, V., Dos Santos, F., et al.: Unprecedented evidence for deep convection hydrating the tropical stratosphere, Geophysical Research Letters, 35, 2008.

Davis, S. M., Liang, C. K., and Rosenlof, K. H.: Interannual variability of tropical tropopause layer clouds, Geophysical Research Letters, 40, 2862–2866, 2013.

Dee, D., Uppala, S., Simmons, A., Berrisford, P., Poli, P., Kobayashi, S., Andrae, U., Balmaseda, M., Balsamo, G., Bauer, P., et al.: The ERA-Interim reanalysis: Configuration and performance of the data assimilation system, Quarterly Journal of the Royal Meteorological Society, 137, 553–597, 2011.

Dessler, A. and Sherwood, S.: Effect of convection on the summertime extratropical lower stratosphere, Journal of Geophysical Research: Atmospheres, 109, 2004.

Dessler, A., Hanisco, T., and Fueglistaler, S.: Effects of convective ice lofting on H_2O and HDO in the tropical tropopause layer, Journal of Geophysical Research: Atmospheres, 112, 2007.

Dessler, A., Schoeberl, M., Wang, T., Davis, S., and Rosenlof, K.: Stratospheric water vapor feedback, Proceedings of the National Academy of Sciences, 110, 18 087–18 091, 2013.

Dessler, A., Schoeberl, M., Wang, T., Davis, S., Rosenlof, K., and Vernier, J.-P.: Variations of stratospheric water vapor over the past three decades, Journal of Geophysical Research: Atmospheres, 119, 2014.

Dessler, A., Ye, H., Wang, T., Schoeberl, M., Oman, L., Douglass, A., Butler, A., Rosenlof, K., Davis, S., and Portmann, R.: Transport of ice into the stratosphere and the humidification of the stratosphere over the 21st century, Geophysical Research Letters, 2016.

Dhomse, S., Weber, M., and Burrows, J.: The relationship between tropospheric wave forcing and tropical lower stratospheric water vapor, Atmospheric Chemistry and Physics, 8, 471–480, 2008.

Frey, W., Schofield, R., Hoor, P., Kunkel, D., Ravegnani, F., Ulanovsky, A., Viciani, S., D'amato, F., and Lane, T.: The impact of overshooting deep convection on local transport and mixing in the tropical upper troposphere/lower stratosphere (UTLS), Atmospheric Chemistry and Physics, 15, 6467–6486, 2015.

Fueglistaler, S. and Haynes, P.: Control of interannual and longer-term variability of stratospheric water vapor, Journal of Geophysical Research: Atmospheres, 110, 2005.

Fueglistaler, S., Dessler, A., Dunkerton, T., Folkins, I., Fu, Q., and Mote, P. W.: Tropical tropopause layer, Reviews of Geophysics, 47, 2009.

Fueglistaler, S., Abalos, M., Flannaghan, T. J., Lin, P., and Randel, W. J.: Variability and trends in dynamical forcing of tropical lower stratospheric temperatures, Atmospheric Chemistry and Physics, 14, 13 439–13 453, 2014.

Geller, M. A., Zhou, X., and Zhang, M.: Simulations of the interannual variability of stratospheric water vapor, Journal of the Atmospheric Sciences, 59, 1076–1085, 2002.

Gettelman, A., Liu, X., Ghan, S. J., Morrison, H., Park, S., Conley, A., Klein, S. A., Boyle, J., Mitchell, D., and Li, J.-L.: Global simulations of ice nucleation and ice supersaturation with an improved cloud scheme in the Community Atmosphere Model, Journal of Geophysical Research: Atmospheres, 115, 2010.

Gilford, D. M., Solomon, S., and Portmann, R. W.: Radiative impacts of the 2011 abrupt drops in water vapor and ozone in the tropical tropopause layer, Journal of Climate, 29, 595–612, 2016.

Giorgetta, M. A. and Bengtsson, L.: Potential role of the quasi-biennial oscillation in the stratosphere-troposphere exchange as found in water vapor in general circulation model experiments, Journal of Geophysical Research: Atmospheres, 104, 6003–6019, 1999.

Hassim, M. and Lane, T.: A model study on the influence of overshooting convection on TTL water vapour, Atmospheric Chemistry and Physics, 10, 9833–9849, 2010.

Herman, R. L., Ray, E. A., Rosenlof, K. H., Bedka, K. M., Schwartz, M. J., Read, W. G., Troy, R. F., Chin, K., Christensen, L. E., Fu, D., Stachnik, R. A., Bui, T. P., and Dean-Day, J. M.: Enhanced stratospheric water vapor over the summertime continental United States and the role of overshooting convection, Atmospheric Chemistry and Physics, 17, 6113, 2017.

Holton, J. R. and Gettelman, A.: Horizontal transport and the dehydration of the stratosphere, Geophysical Research Letters, 28, 2799–2802, 2001.

Hu, D., Tian, W., Guan, Z., Guo, Y., and Dhomse, S.: Longitudinal asymmetric trends of tropical cold-point tropopause temperature and their link to strengthened walker circulation, Journal of Climate, 29, 7755–7771, 2016.

Khaykin, S., Pommereau, J.-P., Korshunov, L., Yushkov, V., Nielsen, J., Larsen, N., Christensen, T., Garnier, A., Lukyanov, A., and Williams, E.: Hydration of the lower stratosphere by ice crystal geysers over land convective systems, Atmospheric Chemistry and Physics, 9, 2275–2287, 2009.

Konopka, P., Ploeger, F., Tao, M., and Riese, M.: Zonally resolved impact of ENSO on the stratospheric circulation and water vapor entry values, Journal of Geophysical Research: Atmospheres, 121, 2016.

Lambert, A., Read, W., Livesey, N., Santee, M., Manney, G., Froidevaux, L., Wu, D., Schwartz, M., Pumphrey, H., Jimenez, C., et al.: Validation of the Aura Microwave Limb Sounder middle atmosphere water vapor and nitrous oxide measurements, Journal of Geophysical Research: Atmospheres, 112, 2007.

Lee, J., Yang, P., Dessler, A. E., Gao, B.-C., and Platnick, S.: Distribution and radiative forcing of tropical thin cirrus clouds, Journal of the Atmospheric Sciences, 66, 3721–3731, 2009.

Liang, C., Eldering, A., Gettelman, A., Tian, B., Wong, S., Fetzer, E., and Liou, K.: Record of tropical interannual variability of temperature and water vapor from a combined AIRS-MLS data set, Journal of Geophysical Research: Atmospheres, 116, 2011.

Liess, S. and Geller, M. A.: On the relationship between QBO and distribution of tropical deep convection, Journal of Geophysical Research: Atmospheres, 117, 2012.

Livesey, N. J., Read, W. G., Wagner, P. A., Froidevaux, L., Lambert, A., Manney, G. L., Millán-Valle, L. F., Pumphrey, H. C., Santee, M. L., Schwartz, M. J., Wang, S., Fuller, R. A., Jarnot, R. F., Knosp, B. W., and Martinez, E.: Earth Observing System (EOS) Aura Microwave Limb Sounder (MLS), Version 4.2x Level 2 data quality and description document, Tech. Rep. JPL D-33509, Tech. Rep. version 4.2x-3.0, NASA Jet Propulsion Laboratory, 2017.

Molod, A., Takacs, L., Suarez, M., Bacmeister, J., Song, I.-S., and Eichmann, A.: The GEOS-5 atmospheric general circulation model: Mean climate and development from MERRA to Fortuna, Technical Report Series on Global Modeling and Data Assimilation Volume 28, NASA Goddard Space Flight Center, 2012.

Mote, P. W., Rosenlof, K. H., McIntyre, M. E., Carr, E. S., Gille, J. C., Holton, J. R., Kinnersley, J. S., Pumphrey, H. C., Russell, J. M., and Waters, J. W.: An atmospheric tape recorder: The imprint of tropical tropopause temperatures on stratospheric water vapor, Journal of Geophysical Research: Atmospheres, 101, 3989–4006, 1996.

Murphy, D. and Koop, T.: Review of the vapour pressures of ice and supercooled water for atmospheric applications, Quarterly Journal of the Royal Meteorological Society, 131, 1539–1565, 2005.

Oman, L. D. and Douglass, A. R.: Improvements in total column ozone in GEOSCCM and comparisons with a new ozone-depleting substances scenario, Journal of Geophysical Research: Atmospheres, 119, 5613–5624, 2014.

Pawson, S., Stolarski, R. S., Douglass, A. R., Newman, P. A., Nielsen, J. E., Frith, S. M., and Gupta, M. L.: Goddard Earth Observing System chemistry-climate model simulations of stratospheric ozone-temperature coupling between 1950 and 2005, Journal of Geophysical Research: Atmospheres, 113, 2008.

Pfister, L., Selkirk, H. B., Jensen, E. J., Schoeberl, M. R., Toon, O. B., Browell, E. V., Grant, W. B., Gary, B., Mahoney, M. J., Bui, T. V., and Hintsa, E.: Aircraft observations of thin cirrus clouds near the tropical tropopause, Journal of Geophysical Research: Atmospheres, 106, 9765–9786, 2001.

Plumb, R. A. and Bell, R. C.: A model of the quasi-biennial oscillation on an equatorial beta-plane, Quarterly Journal of the Royal Meteorological Society, 108, 335–352, 1982.

Randel, W. J. and Jensen, E. J.: Physical processes in the tropical tropopause layer and their roles in a changing climate, Nature Geoscience, 6, 169–176, 2013.

Randel, W. J., Wu, F., and Gaffen, D. J.: Interannual variability of the tropical tropopause derived from radiosonde data and NCEP reanalyses, Journal of Geophysical Research: Atmospheres, 105, 15–509, 2000.

Randel, W. J., Wu, F., Voemel, H., Nedoluha, G. E., and Forster, P.: Decreases in stratospheric water vapor after 2001: Links to changes in the tropical tropopause and the Brewer-Dobson circulation, Journal of Geophysical Research: Atmospheres, 111, 2006.

Read, W., Lambert, A., Bacmeister, J., Cofield, R., Christensen, L., Cuddy, D., Daffer, W., Drouin, B., Fetzer, E., Froidevaux, L., et al.: Aura Microwave Limb Sounder upper tropospheric and lower stratospheric H_2O and relative humidity with respect to ice validation, Journal of Geophysical Research: Atmospheres, 112, 2007.

Schiller, C., Grooß, J.-U., Konopka, P., Plöger, F., Silva dos Santos, F., and Spelten, N.: Hydration and dehydration at the tropical tropopause, Atmospheric Chemistry and Physics, 9, 9647–9660, 2009.

Schoeberl, M. and Dessler, A.: Dehydration of the stratosphere, Atmospheric Chemistry and Physics, 11, 8433–8446, 2011.

Schoeberl, M., Dessler, A., and Wang, T.: Simulation of stratospheric water vapor and trends using three reanalyses, Atmospheric Chemistry and Physics, 12, 6475–6487, 2012.

Schoeberl, M., Dessler, A., and Wang, T.: Modeling upper tropospheric and lower stratospheric water vapor anomalies, Atmospheric Chemistry and Physics, 13, 7783–7793, 2013.

Schoeberl, M. R., Dessler, A. E., Wang, T., Avery, M. A., and Jensen, E. J.: Cloud formation, convection, and stratospheric dehydration, Earth and Space Science, 1, 1–17, 2014.

Schwartz, M. J., Read, W. G., Santee, M. L., Livesey, N. J., Froidevaux, L., Lambert, A., and Manney, G. L.: Convectively injected water vapor in the North American summer lowermost stratosphere, Geophysical Research Letters, 40, 2316–2321, 2013.

Sherwood, S. C. and Dessler, A. E.: On the control of stratospheric humidity, Geophysical Research Letters, 27, 2513–2516, 2000.

Smalley, K. M., Dessler, A. E., Bekki, S., Deushi, M., Marchand, M., Morgenstern, O., Plummer, D. A., Shibata, K., Yamashita, Y., and Zeng, G.: Contribution of different processes to changes in tropical lower-stratospheric water vapor in chemistry–climate models, Atmospheric Chemistry and Physics, 17, 8031–8044, 2017.

Solomon, S., Rosenlof, K. H., Portmann, R. W., Daniel, J. S., Davis, S. M., Sanford, T. J., and Plattner, G.-K.: Contributions of stratospheric water vapor to decadal changes in the rate of global warming, Science, 327, 1219–1223, 2010.

Stenke, A. and Grewe, V.: Simulation of stratospheric water vapor trends: impact on stratospheric ozone chemistry, Atmospheric Chemistry and Physics, 5, 1257–1272, 2005.

Sun, Y. and Huang, Y.: An examination of convective moistening of the lower stratosphere using satellite data, Earth and Space Science, 2, 320–330, 2015.

Tao, M., Konopka, P., Ploeger, F., Riese, M., Müller, R., and Volk, C. M.: Impact of stratospheric major warmings and the quasi-biennial oscillation on the variability of stratospheric water vapor, Geophysical Research Letters, 42, 4599–4607, 2015.

Ueyama, R., Jensen, E. J., Pfister, L., Diskin, G. S., Bui, T., and Dean-Day, J. M.: Dehydration in the tropical tropopause layer: A case study for model evaluation using aircraft observations, Journal of Geophysical Research: Atmospheres, 119, 5299–5316, 2014.

Ueyama, R., Jensen, E. J., Pfister, L., and Kim, J.-E.: Dynamical, convective, and microphysical control on wintertime distributions of water vapor and clouds in the tropical tropopause layer, Journal of Geophysical Research: Atmospheres, 120, 2015.

Virts, K. S. and Houze Jr, R. A.: Clouds and water vapor in the tropical tropopause transition layer over mesoscale convective systems, Journal of the Atmospheric Sciences, 72, 4739–4753, 2015.

Wang, T. and Dessler, A. E.: Analysis of cirrus in the tropical tropopause layer from CALIPSO and MLS data: A water perspective, Journal of Geophysical Research: Atmospheres, 117, 2012.

Wang, T., Randel, W., Dessler, A., Schoeberl, M., and Kinnison, D.: Trajectory model simulations of ozone (O_3) and carbon monoxide (CO) in the lower stratosphere, Atmospheric Chemistry and Physics, 14, 7135–7147, 2014.

Wang, W., Matthes, K., and Schmidt, T.: Quantifying contributions to the recent temperature variability in the tropical tropopause layer, Atmospheric Chemistry and Physics, 15, 5815–5826, 2015.

Wright, J., Fu, R., Fueglistaler, S., Liu, Y., and Zhang, Y.: The influence of summertime convection over Southeast Asia on water vapor in the tropical stratosphere, Journal of Geophysical Research: Atmospheres, 116, 2011.

Wright, J. S., Sobel, A. H., and Schmidt, G. A.: Influence of condensate evaporation on water vapor and its stable isotopes in a GCM, Geophysical Research Letters, 36, 2009.

Yulaeva, E., Holton, J. R., and Wallace, J. M.: On the cause of the annual cycle in tropical lower-stratospheric temperatures, Journal of the Atmosperic Sciences, 51, 169–174, 1994.

Zhou, C., Dessler, A., Zelinka, M., Yang, P., and Wang, T.: Cirrus feedback on interannual climate fluctuations, Geophysical Research Letters, 41, 9166–9173, 2014.

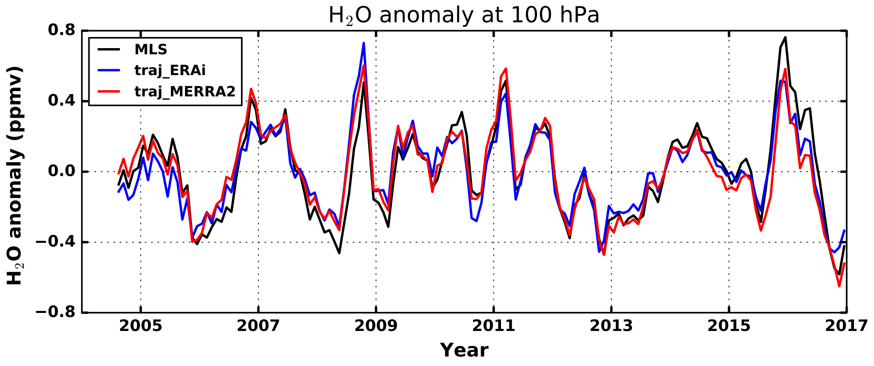

Figure 1. Tropical (30°N-30°S) monthly water vapor anomalies at 100 hPa from MLS observations (black line) and from trajectory model runs driven by ERAi (blue line) and MERRA-2 (red line) from August 2004 through 2016. Anomalies are calculated by subtracting the mean annual cycle from the observations.

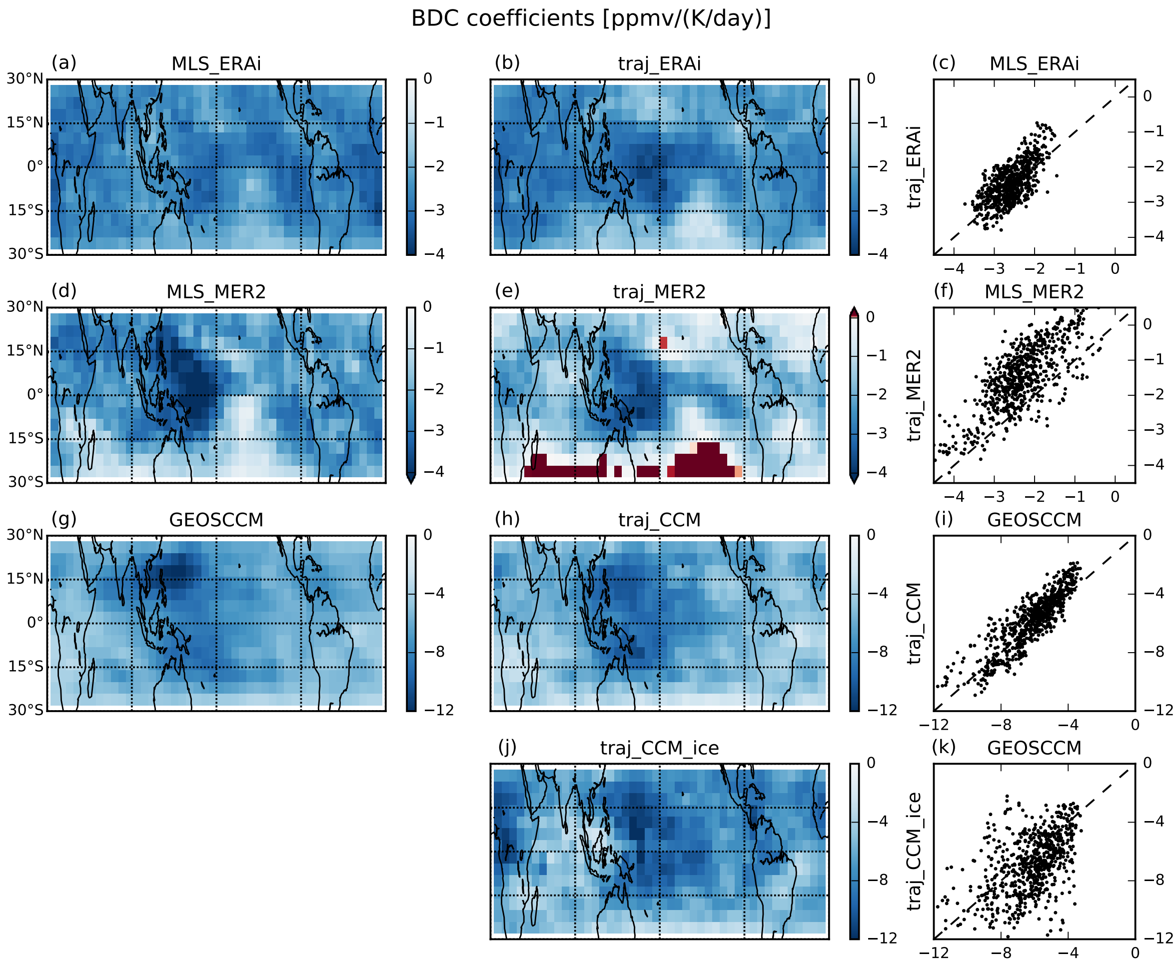

Figure 2. Multivariate linear regression coefficients of the BDC regressor from MLS and GEOSCCM H_2O fields (left column), as well as the coefficients from regression of the associated trajectory model fields (middle column). Scatter plots of MLS/GEOSCCM regressions vs. trajectory model regressions indicate the similarity of the fields (right column). The MLS and associated trajectory regressions cover the period August 2004 to December 2016 between 30°N and 30°S. The GEOSCCM and associated trajectory run cover 2005-2016 model years. The bottom row shows coefficients from regressions of a run of the trajectory model driven by GEOSCCM meteorology that includes evaporation of convective ice.

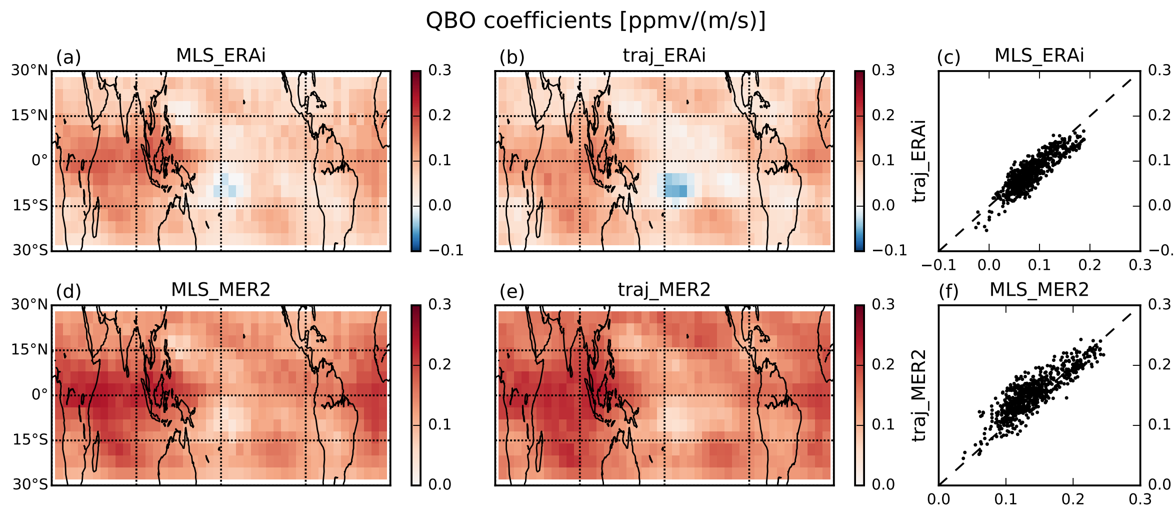

Figure 3. Same as Fig. 2, but for coefficients of the QBO regressor.

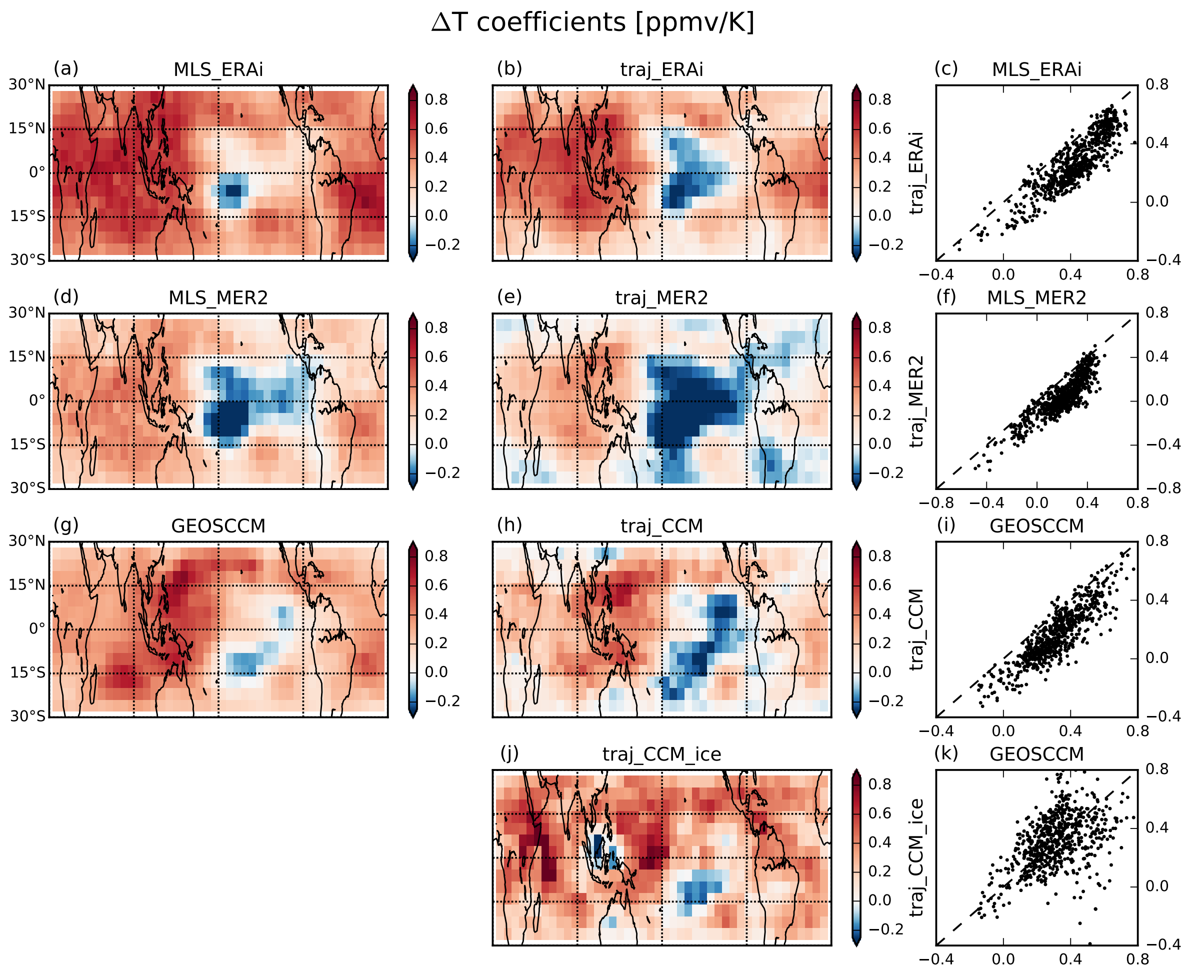

Figure 4. Same as Fig. 2, but for the coefficient of the ΔT regressor.

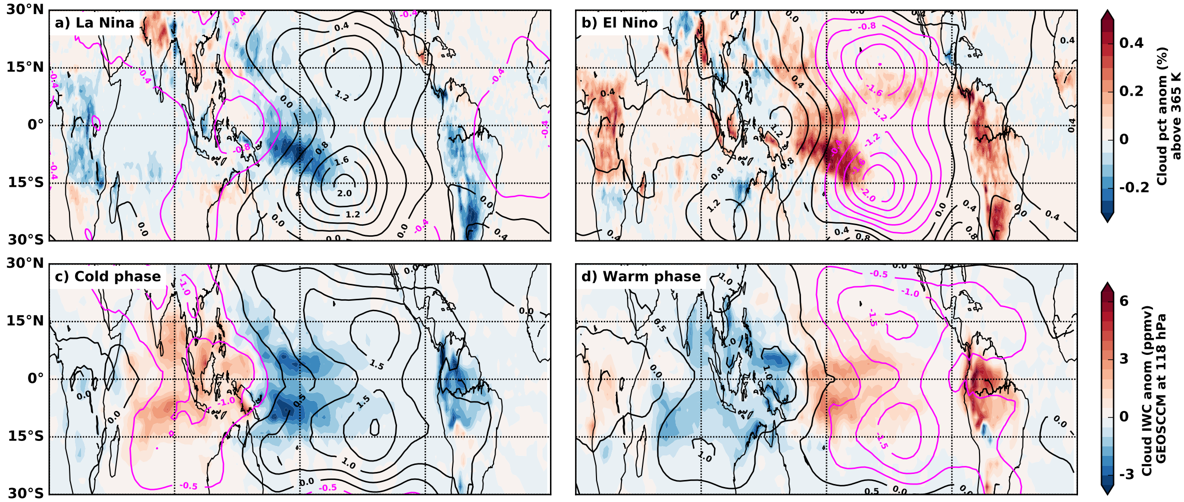

Figure 5. Averaged monthly cloud occurrence frequency anomalies above 365 K during (a) La Niña and (b) El Niño months from 2005 to 2016; also shown as contours are temperature anomalies at 100 hPa. La Niña and El Niño months are based on the NOAA Oceanic Niño Index (ONI) in the Niño 3.4 region (5°S to 5°N; 170°W to 120°W). Averaged monthly GEOSCCM convective cloud ice water content (IWC) anomalies (ppmv) at 118 hPa during (c) cold and (d) warm GEOSCCM phases from model years 2005 to 2016 with averaged temperature anomalies at 100 hPa shown as contours. The cold and warm phases are defined to be GEOSCCM surface temperature anomaly (departures from the mean annual cycle) of +0.5 K and -0.5 K, respectively, in the Niño 3.4 region (same as ONI).

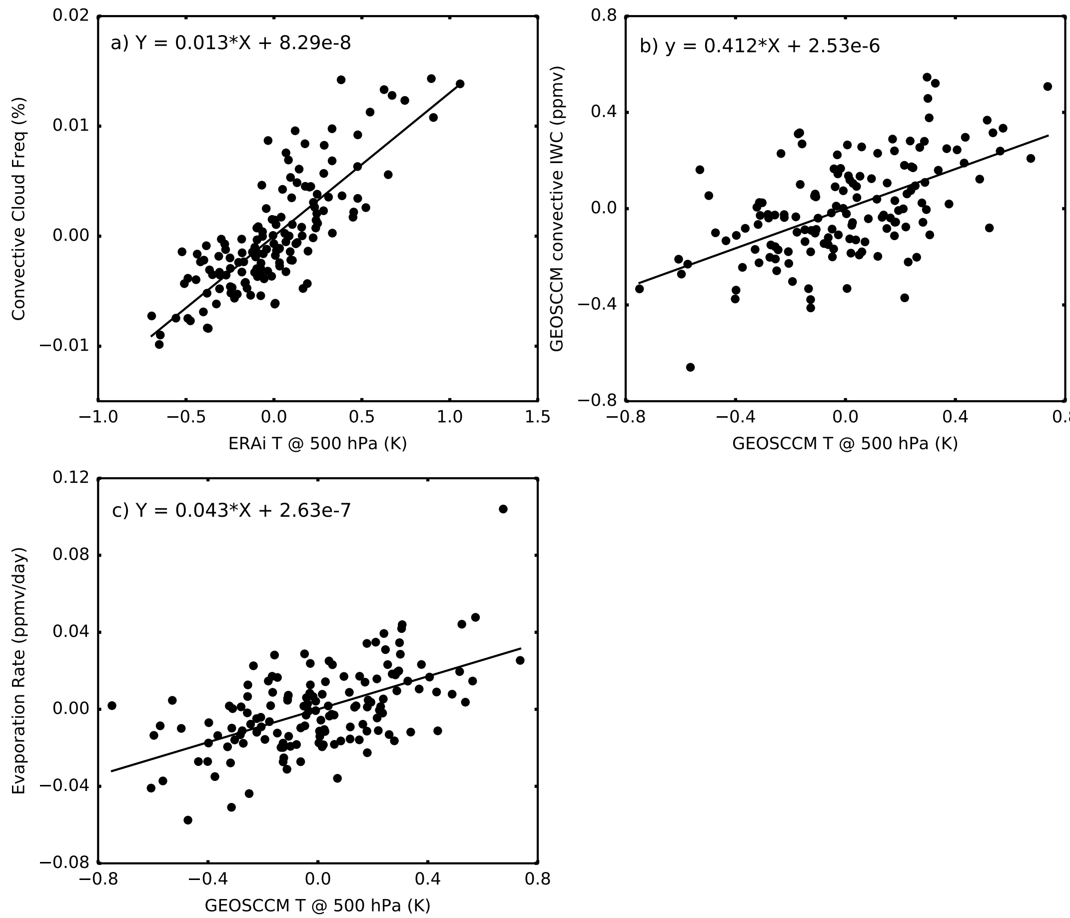

Figure 6. (a) Observed convective cloud occurrence frequency anomalies at 370 K and 500-hPa ΔT from ERAi. (b) Convective IWC anomalies at 118 hPa and ΔT from GEOSCCM. (c) GEOSCCM convective cloud evaporation rate anomalies at 100 hPa and ΔT. All the data is monthly and tropical averaged from 30°S to 30°N.

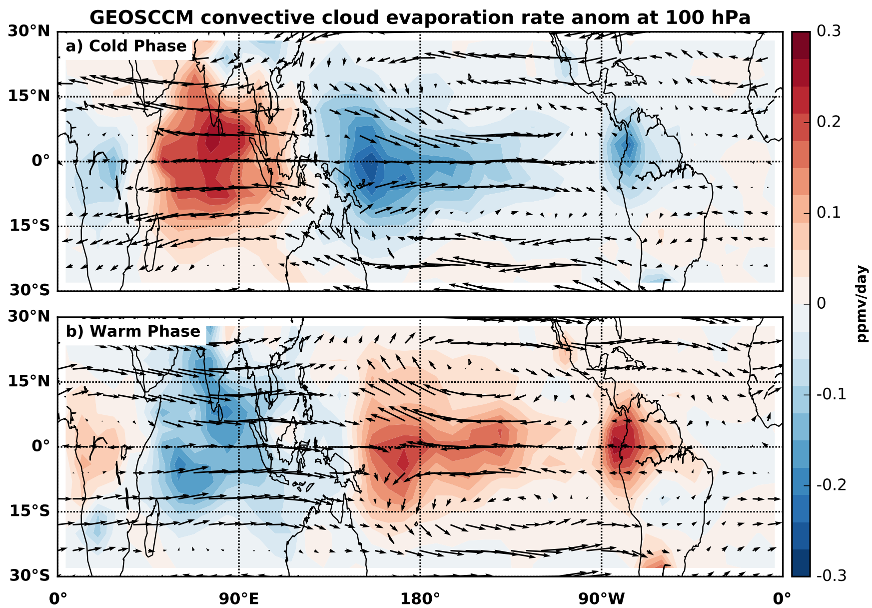

Figure 7. Averaged monthly GEOSCCM convective cloud evaporation rate anomalies at 100 hPa during (a) warm and (b) cold GEOSCCM phases from 2005 to 2016. Also shown are averaged horizontal wind anomaly vectors at 100 hPa.